Order−Disorder Transformation in $RuBr_3$ and $MoBr_3$: A Two-Dimensional Ising Model

Stefano Merlino

Dipartimento di Scienze della Terra, Università di Pisa, via S. Maria 53, 56126 Pisa, Italy

Luca Labella, Fabio Marchetti,* and Simone Toscani

Dipartimento di Chimica e Chimica Industriale, Università di Pisa, via Risorgimento 35, 56126 Pisa, Italy

Received May 14, 2004. Revised Manuscript Received June 22, 2004

Several trihalides (Cl, Br, I) of elements of groups 4, 5, 6, and 8 of the periodic table, such as TiI_3, show a crystal structure made by parallel infinite columns, running along **c**, of face-sharing octahedra [MX_6]. The metals placed within the columns may interact with one of the nearest neighbors, so that long and short MM distances regularly alternate along the columns; two distinct conformations are possible for the columns, one with M−M pairs centered at $z = 1/4$, the other with M−M pairs centered at $z = 3/4$. Below a certain temperature the distribution of the two types of columns in the **a**,**b** plane is ordered, giving rise to an orthorhombic form, with space group *Pnmm*. Over this temperature a transition to a hexagonal form, with space group $P6_3/mcm$, is observed. We, through X-ray diffraction studies carried out at different temperatures, estimate this transition temperature for $RuBr_3$ and $MoBr_3$ crystals and show that the hexagonal form too consists of ordered columns, the higher symmetry of that phase being due to a random distribution of the two types of columns in the **a**,**b** plane. We suggest that an equal spanning of the metals in the columns, as proposed by previous authors for the hexagonal phase, is never realized in any compound with the TiI_3 structure type and present a possible mechanism of the order−disorder phase transition in this class of compounds and discuss it within the frame of a two-dimensional Ising model.

1. Introduction

A large number of metals in the second and third transition series form trihalides (apart from trifluorides) with the structure type of TiI_3: (d^1) $ZrCl_3$, $ZrBr_3$, ZrI_3, HfI_3; (d^2) NbI_3; (d^3) $MoBr_3$, MoI_3; (d^5) β-$RuCl_3$, $RuBr_3$, RuI_3, OsI_3; (d^{10}) InI_3.[1] This structure type, first found in TiI_3,[2] is characterized by the presence of columns $MX_{6/2}]_1^\infty$ of face-sharing octahedra [MX_6]: the columns run along the **c** axis and are arranged in the **a**,**b** plane as represented in Figure 1.

The structures of these compounds were first assigned to the hexagonal space group $P6_3/mcm$ with one chain per unit cell and equidistant metals along the chains. However, several studies pointed to the presence of additional X-ray reflections violating the systematic absences of the $P6_3/mcm$ symmetry [Holze (zirconium trihalides);[2] von Schnering, (TiI_3)].[3] Later on, Brodersen et al.[4] showed that $RuBr_3$ crystals display the TiI_3 structure type with orthorhombic space group *Pnmm* ($a_O = a_H$, $b_O = (\sqrt{3})b_H$, $c_O = c_H$; the O and H subscripts refer to the orthorhombic cell and the corresponding hexagonal cell, respectively), with two chains per unit cell. The metal atoms in the chains running along *c* are no more constrained to be equidistant and may form metal pairs with alternating short Ru−Ru and long Ru···Ru distances, 2.73 and 3.13 Å, respectively.[4] The two chains running in the unit cell are crystallographi-

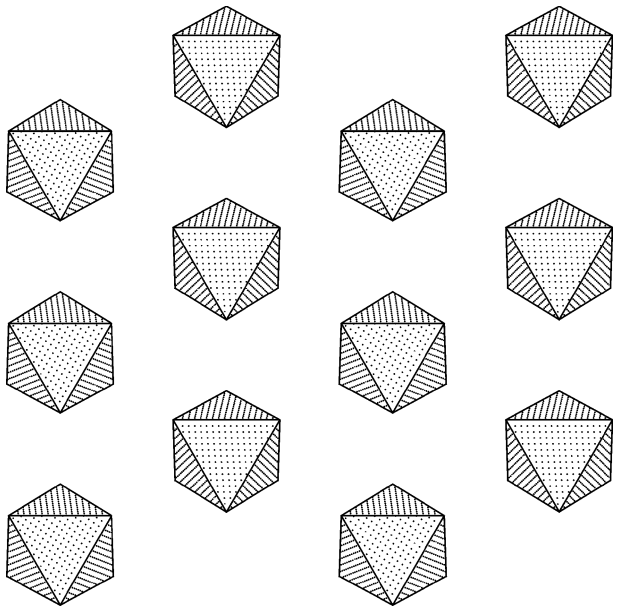

Figure 1. Projection along **c** of the column layout in the TiI_3 structure type.

* To whom correspondence should be addressed. E-mail fama@dcci.unipi.it.

(1) Lin, J.; Miller, G. J. *Inorg. Chem.* **1993**, *32*, 1476.
(2) Holze, E. Dissertation, Westfälische Wilhelms Universität, Münster, Germany, 1956.
(3) von Schnering, H. G. *Naturwissenschaften* **1966**, *53*, 359.
(4) Brodersen, K.; Breitbach, H.-K.; Thiele, G. *Z. Anorg. Allg. Chem.* **1968**, *357*, 162.

10.1021/cm049235q CCC: $27.50
Published on Web 09/09/2004

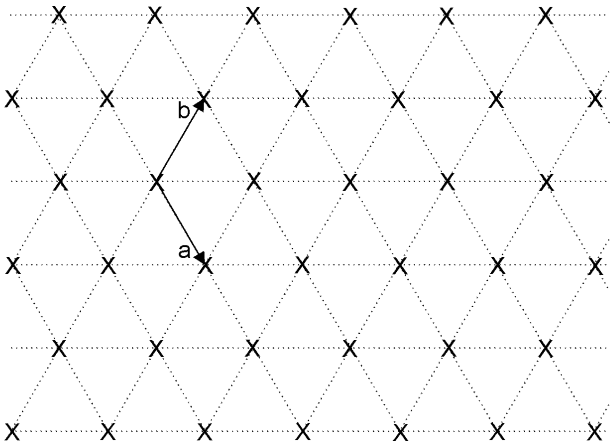

Figure 2. Schematic representation in the **a**,**b** plane of chains $[MX_{6/2}]_1^\infty$ with equally spanned metals placed at $z = 0$ and $z = 1/2$. The hexagonal unit cell is indicated.

cally equivalent and related through the *n* glide normal to **a**, so that whereas in one chain the Ru−Ru short distance is centered at $z = 1/4$, in the other chain it is centered at $z = 3/4$.

Similarly, the *Pnmm* space group symmetry has been subsequently found by Babel in $MoBr_3$,[5] by Hillebrecht et al. in MoI_3 and OsI_3,[6] and by Lachgar et al. in ZrI_3,[7] in all cases through single-crystal X-ray investigations.

Before describing the structural details of the orthorhombic arrangement of the TiI_3 structure type (see the section on the structural study), we introduce a simple scheme illustrating its distinctive features with respect to the hexagonal arrangement and present our view on the relationships between the two structural forms.

In the hexagonal arrangement all the columns are translationally equivalent with equidistant metal atoms placed at $z = 0$ and $z = 1/2$. The distribution of the chains (which will be denoted with the symbol X) in the **a**,**b** plane is described in Figure 2.

However, there is another possible model consistent with the $P6_3/mcm$ space group symmetry. With localized M−M bonds and formation of metal pairs along the chain, regular alternation of short M−M and M···M distances will occur. This regular alternation may be realized in two distinct ways: the short distance may be centered at $z = 1/4$ (the corresponding conformation will be denoted +) or at $z = 3/4$ (the corresponding conformation will be denoted −). A structure with a random distribution of the two kinds of chains in a "triangular" net in the **a**,**b** plane (this random distribution is denoted through the symbol ± in Figure 3) should afford a diffraction pattern closely similar to that displayed by the structure schematically described in Figure 2. In fact, the metal atoms are now randomly located, in positions slightly higher than $z = 0$ and slightly lower than $z = 1/2$ (conformation +) or in positions slightly lower than $z = 0$ and slightly higher than $z = 1/2$ (conformation −): the diffraction pattern will point to the average positions $z = 0$ and $z = 1/2$.

Most likely, such random distribution in a structure with $P6_3/mcm$ space group symmetry will occur for all

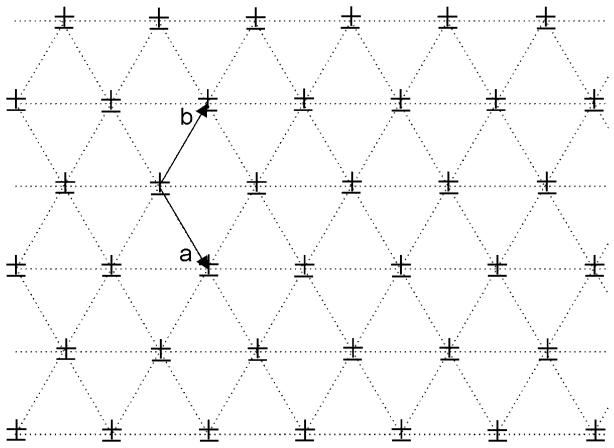

Figure 3. Schematic representation in the **a**,**b** plane of chains $[MX_{6/2}]_1^\infty$ with alternating long and short MM distances with a random distribution of the two types of chains. The hexagonal unit cell is indicated. The symbol + represents the chains with the M−M pairs centered at $z = 1/4$, and the symbol − represents the chains with the M−M pairs centered at $z = 3/4$.

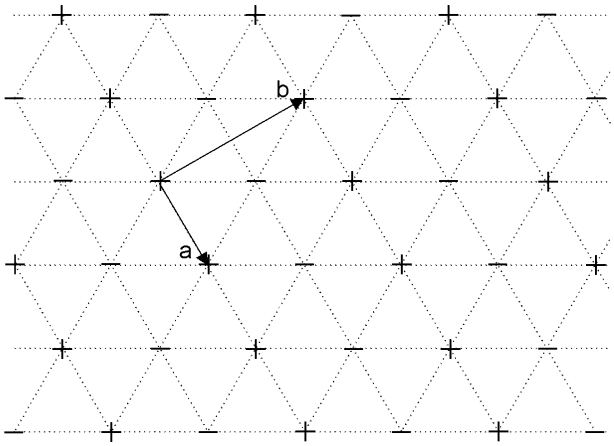

Figure 4. Schematic representation in the **a**,**b** plane of chains $[MX_{6/2}]_1^\infty$ with alternating long and short MM distances with an ordered distribution of chains. The orthorhombic unit cell is indicated. The symbol + represents the chains with the M−M pairs centered at $z = 1/4$, and the symbol − represents the chains with the M−M pairs centered at $z = 3/4$.

the trihalides with the structure type of TiI_3 at sufficiently high temperature (for some of them even at room temperature). At sufficiently low temperature the octahedral chains will distribute themselves more orderly in the **a**,**b** plane, with descent to space group symmetry *Pnmm* and appearance of additional reflections, characteristic of the orthorhombic phase of the TiI_3 structure type. In the limit of complete order the distribution of the + and − columns would correspond to the scheme presented in Figure 4.

Namely, we maintain that in all those trihalides the single chains are fully ordered, with + or − conformations, and that the hexagonal ($P6_3/mcm$) and orthorhombic (*Pnmm*) arrangements correspond, respectively, to the disordered and ordered distributions of the internally ordered chains. The transformation from the ordered to the disordered state should be a continuous one, with the degree of order progressively decreasing with increasing temperature.

Figure 5 represents the diffraction pattern (actually the plane *hk*0 of the reciprocal lattice) for the orthor-

(5) Babel, D. *J. Solid State Chem.* **1972**, *4*, 410.
(6) Hillebrecht, H.; Rotter, H.; Thiele, G. *Z. Kristallogr.* **1989**, *2* (Suppl. 2), 74.
(7) Lachgar, A.; Dudis, D. S.; Corbett, J. D. *Inorg. Chem.* **1990**, *29*, 2242.

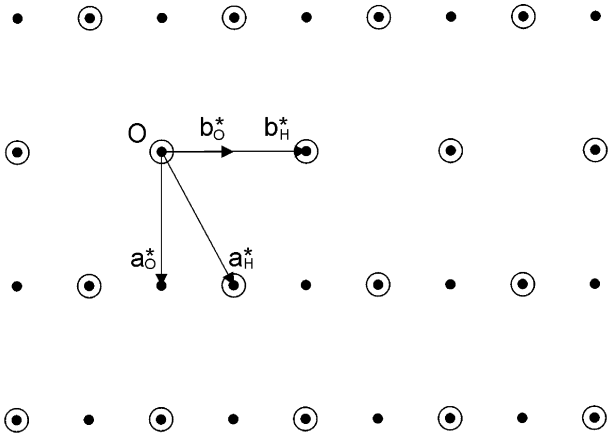

Figure 5. *hk*0 diffraction pattern for the TiI_3 structure type with different ordering in the chains. The symbols ● and ○ indicate the orthorhombic and hexagonal reflections, respectively.

hombic (small filled circles) and hexagonal (large open circles) structures. It is evident that the reflections with $h + k = 2n$ are common to both structures and will be indicated as "structure" reflections (thereafter, unless specified, we shall use unsubscripted indices *h*, *k*, and *l* when we refer to the orthorhombic cell), whereas the reflections with $h + k = 2n + 1$ are characteristic for the ordered structure and will be indicated as "superstructure" reflections. The latter reflections will appear when the ordering sets up, and their intensity will obviously increase with the order parameter.

As the two columns in the unit cell of the orthorhombic structure are symmetry-equivalent in the space group *Pnmm*, the macroscopic order parameter *Q* is simply given by $|x(+) - x(-)|$ for one of the two columns, $x(+)$ and $x(-)$ indicating the fraction of + and − conformations for that column.

The order parameter *Q*, which is proportional to the square root of the intensity *I* of the superstructure reflections, assumes the value 1 for the fully ordered "orthorhombic" phase at low temperature (ideally at 0 K) and the value 0 for the high-temperature "hexagonal" phase. Its dependence on temperature is given by the expression

$$\sqrt{I} \propto Q = |(T - T_c)/T_c|^{\beta}$$

where T_c is the critical temperature and β is the critical exponent.

The aim of the present work is to collect experimental evidence to support the validity of the model just presented, through X-ray structural investigations on single crystals of $RuBr_3$ and $MoBr_3$, measurements of the variation of the degree of order with rising temperature, determination of the critical temperatures for the two compounds, and discussion of the results within the frame of a two-dimensional Ising model.[8]

2. Sample Preparation and Room Temperature X-ray Studies

$RuBr_3$ was prepared by a two-step bromination of $Ru_3(CO)_{12}$: the first step at low temperature produces a mixture of $Ru_2(CO)_6Br_4$ and $Ru(CO)_4Br_2$; the second one at high temperature produces $RuBr_3$.

Bromination of $Ru_3(CO)_{12}$ at Low Temperature. Under an Ar atmosphere 5.009 g of $Ru_3(CO)_{12}$ (7.84 mmol) was slowly added to 3 mL of Br_2 (58 mmol) kept at 16 °C by a water bath. When the $CO_{(g)}$ evolution ceased, the excess of bromine was removed under reduced pressure (3 h, 5×10^{-2} Torr). The solid product was washed with anhydrous heptane (30 mL), filtered, and dried in vacuo at room temperature. The IR spectrum in a N_2 atmosphere (Nujol mull and CaF_2 windows) showed five carbonylic bands (cm^{-1}): 2021w, 2095s, 2117s, 2132s, 2183m, attributable to a mixture of $Ru_2(CO)_6Br_4$[8] and $Ru(CO)_4Br_2$.[8] On the basis of the carbon percentage found by elemental analysis (11.82), the $Ru_2(CO)_6Br_4/Ru(CO)_4Br_2$ molar ratio has been estimated to be 43/57.

Bromination of a Ruthenium Carbonyl Bromide Mixture at High Temperature. A 0.591 mg sample of the product of the previous reaction (1.64 mmol of Ru atoms) was put in the middle of a silica glass pipe placed in a tubular furnace. The device was closed and repeatedly subjected to vacuum/Ar cycles, then the temperature was raised to 280 °C, and a slow flow of bromine vapors driven by Ar was passed through the open pipe for 3 h. A volume of about 5 mL (97 mmol) of $Br_{2(l)}$ was vaporized and brought into contact with the solid. The temperature was then left to decrease to the room value with a continuous Ar flow to remove the unreacted bromine vapors. At room temperature the black powder obtained was collected in air. The elemental analysis indicated 0.29% C. The IR spectrum (Nujol mull and CaF_2 windows) showed no bands in the 1500−2400 cm^{-1} region. The X-ray diffraction pattern of the polycrystalline sample clearly corresponded, apart from the peak width, to the pattern calculated on the basis of the known structural data of $RuBr_3$.[4]

Growth of $RuBr_3$ Crystals. A 18.2 mg sample of $RuBr_3$ under 1 atm of Ar saturated by Br_2 vapors was introduced at the bottom of a silica glass tube (10 mm $\varnothing_{int}$, 14 mm $\varnothing_{ext}$, 70 mm long) which was then flame sealed. The tube was put into a furnace with the end containing the powder in a zone at 690 ± 5 °C and the opposite end in a zone at 630 ± 5 °C. The crystals grew at the colder end as thin needles in about 25 days.

Preparation and Growth of $MoBr_3$ Crystals. $MoBr_3$ was prepared from the elements following the literature.[10] The reaction, carried out in a sealed tube, directly afforded single crystals. A 25.0 mg sample of powdered Mo (0.261 mmol) and 128 mg (0.804 mmol) of liquid Br_2 under an Ar atmosphere were introduced at the bottom of a silica glass tube (10 mm $\varnothing_{int}$, 14 mm $\varnothing_{ext}$, 70 mm long). The tube end containing the reagents was cooled in liquid N_2, the Ar was evacuated, and the tube was sealed. Then it was put into a tubular furnace with the end containing the reagents in a zone at 360 ± 5 °C and the opposite one in a zone at 322 ± 5 °C. The crystals grew at the colder end as thin needles in about 20 days.

Both $RuBr_3$ and $MoBr_3$ single crystals we could grow were very thin needles. Those with suitable thickness were too long (1−2 mm), and any attempt of cutting them resulted in an unraveled end such as a brush. After many unsuccessful attempts to correct the shape of the crystals, we glued needles of suitable thickness at the end of silica fibers, disregarding the excessive length.

The crystals were examined through Weissenberg photographs to select the most suitable ones for intensity data collections and to confirm the space group *Pnmm*. The intensity data were collected for both $RuBr_3$ (untwinned crystal, dimensions $0.26 \times 0.033 \times 0.015$ mm^3) and $MoBr_3$ (the crystal was actually a "Drilling", with the three orthorhombic individuals in an orientation related by 120° rotations about **c**, as

(8) (a) Lenz, W. *Z. Phys.* **1920**, *21*, 613. (b) Ising, E. *Z. Phys.* **1925**, *31*, 253.

(9) (a) Benedetti, E.; Braca, G.; Sbrana, G.; Salvetti F.; Grassi, B. *J. Organomet. Chem.* **1972**, *37*, 361. (b) Johnson, B. F. G.; Johntson, R. D.; Lewis, J. *J. Chem. Soc. A* **1969**, 792. (c) Colton, R.; Farthing, R. H. *Austr. J. Chem.* **1967**, *20*, 1283.

(10) (a) Babel, D.; Rüdorff, W. *Naturwissenschaften* **1964**, *4*, 85. (b) Lewis, J.; Machin, D. J.; Nyholm, R. S.; Pauling, P.; Smith P. W. *Chem. Ind. (London)* **1960**, 259.

Table 1. Data Collection and Refinement of $RuBr_3$ and $MoBr_3$

	$RuBr_3$	$MoBr_3$		$RuBr_3$	$MoBr_3$
wavelength (Å)	0.71073	0.71073	no. of reflns collected	816	867
space group	Pnmm	Pnmm	no. of independent reflns	510 (R_{int} = 0.062)	581 (R_{int} = 0.034)
a (Å)	6.488(1)	6.605(1)	no. of independent reflns [$I > 2\sigma(I)$]	279	346
b (Å)	11.235(3)	11.442(2)	no. of refined params	28	28
c (Å)	5.859(1)	6.077(1)	GOF	1.010	1.176
V (Å^3)	427.07(16)	459.25(11)	R1, wR2 [$I > 2\sigma(I)$]	0.055, 0.116	0.041, 0.081
ρ_{calcd} (g·cm^{-3})	5.30	4.86	R1, wR2 (all data)	0.112, 0.143	0.082, 0.091
μ (mm^{-1})	31.51	28.74	max peak and hole in ΔF (e·Å^{-3})	1.85/−1.77	1.78/−0.902

Table 2. Atomic Coordinates and Equivalent Isotropic Displacement Parameters (Å^3) for the Room Temperature Structure of $RuBr_3$ and $MoBr_3$[a]

	x/a	y/b	z/c	U_{eq}
Ru	0.2550(3)	1/4	0.0168(3)	0.018(1)
Br(1)	0.4075(4)	0.4020(2)	−1/4	0.023(1)
Br(2)	0.0969(4)	0.4088(2)	1/4	0.024(1)
Br(3)	0.5724(5)	1/4	1/4	0.025(1)
Br(4)	−0.0502(5)	1/4	−1/4	0.022(1)
Mo	0.2539(3)	1/4	0.0135(3)	0.022(1)
Br(1)	0.4082(3)	0.4045(2)	−1/4	0.027(1)
Br(2)	0.0931(3)	0.4104(2)	1/4	0.028(1)
Br(3)	0.5727(4)	1/4	1/4	0.028(1)
Br(4)	−0.0573(4)	1/4	−1/4	0.026(1)

[a] U_{eq} is defined as one-third of the trace of the orthogonalized U_{ij} tensor.

Table 3. Anisotropic Displacement Parameters (Å^2) for $RuBr_3$ and $MoBr_3$[a]

	U_{11}	U_{22}	U_{33}	U_{23}	U_{13}	U_{12}
Ru	0.022(1)	0.017(1)	0.016(1)	0	0.000(1)	0
Br(1)	0.030(1)	0.020(1)	0.019(2)	0	0	−0.006(1)
Br(2)	0.033(1)	0.021(1)	0.019(2)	0	0	0.005(1)
Br(3)	0.021(2)	0.036(2)	0.018(2)	0	0	0
Br(4)	0.022(2)	0.025(2)	0.019(2)	0	0	0
Mo	0.018(1)	0.018(1)	0.030(1)	0	−0.002(1)	0
Br(1)	0.032(1)	0.025(1)	0.024(2)	0	0	−0.006(1)
Br(2)	0.035(1)	0.025(1)	0.023(2)	0	0	0.007(1)
Br(3)	0.021(1)	0.039(2)	0.025(2)	0	0	0
Br(4)	0.019(1)	0.035(2)	0.022(2)	0	0	0

[a] The anisotropic displacement factor exponent takes the form $-2\pi^2[h^2(a^*)^2U_{11} + ... + 2hka^*b^*U_{12}]$.

described by Babel,[5] with dimensions 1.55 × 0.14 × 0.07 mm^3) with an automatic single-crystal diffractometer (Bruker P4, graphite-monochromatized Mo Kα radiation). In the case of $MoBr_3$ the data were collected from the largest individual in the Drilling. Moreover, the intensities of the structure reflections ($h + k = 2n$) have been properly rescaled, taking into account that they result from the superposition of the reflections of the three individuals of the Drilling.[5]

Through least-squares refinement of 15 and 36 medium-angle reflections for $RuBr_3$ and $MoBr_3$, respectively, the cell parameters of both compounds have been determined and are reported in Table 1.

The intensities were corrected for Lorentz and polarization factors, as well as for absorption with the ψ-scanning procedure[11] for $RuBr_3$, and by an integration method based on the crystal shape[11] for $MoBr_3$.

The structure refinements were carried out on $|F|^2$ using SHELX-97 programs,[12] starting from the positional parameters found by Brodersen et al.[4] and Babel[5] for $RuBr_3$ and $MoBr_3$, respectively. The final reliability indices, with anisotropic thermal parameters, for reflections with $I > 2\sigma(I)$, were 0.055 and 0.041 for $RuBr_3$ and $MoBr_3$, respectively.

Some details of the data collection and structure refinement are presented in Table 1. The final positional and thermal parameters for both compounds are given in Tables 2 and 3.

3. Structural Features

The relevant bond lengths and bond angles for both $RuBr_3$ and $MoBr_3$ at room temperature are presented in Table 4, whereas the crystal structures are illustrated in Figures 6 and 7.

The main features of these structures have already been described by Brodersen et al.[4] and Babel,[5] as recalled in the Introduction. According to our results, in the infinite columns of [MBr_6] octahedra (M = Ru, Mo) running parallel to c, a regular alternation of short M−M distances (2.732 and 2.874 Å in the Ru and Mo compounds, respectively) and long M···M distances (3.127 and 3.203 Å in the Ru and Mo compounds, respectively) occurs. The bromide anions form nearly equilateral triangles placed between the metal atoms: the triangles placed between the metal atoms of the "short-distance" pair are larger (average Br···Br distances are 3.55 and 3.66 Å in the Ru and Mo compounds, respectively) than those placed between the "long-distance" pair (average Br···Br distances are 3.42 and 3.54 Å in the Ru and Mo compounds, respectively).

The metal atoms in the [MBr_6] octahedra present shorter bonds with bromine atoms of the large triangle (2.470 and 2.557 Å in [$RuBr_6$] and [$MoBr_6$], respectively, with Br−M−Br angles of 92.4° and 91.5° in the Ru and Mo compounds, respectively) and longer bonds with the bromine atoms of the small triangle (2.520 and 2.598 Å in [$RuBr_6$] and [$MoBr_6$], respectively, with Br−M−Br angles of 86.0° in both compounds).

The relative arrangement of the various columns appears from Figure 6, where the "white" and "gray" octahedral columns present the short-distance Ru−Ru pair located at z = 1/4 and z = 3/4, and is further illustrated in Figure 7. The ordered arrangement of the columns and the consequently ordered distribution of small and large bromine triangles in each anionic plane favor a homogeneous assessment of the van der Waals contacts between bromine atoms of adjacent columns, with a limited range of variation of the Br···Br distances, 3.84−3.91 Å in $RuBr_3$ and 3.89−3.96 Å in $MoBr_3$.

4. High-Temperature Study

Crystals of $RuBr_3$ and $MoBr_3$ for the high-temperature studies were first examined through Weissenberg photographs. The selected crystals were heated, step by step, with a high-temperature device connected to a Bruker P4 four-circle diffractometer. The intensities of a pair of superstructure reflections (123 and 413, selected for their relatively high intensities) were measured (two times) at each step. The measured

(11) Sheldrick, G. M. *SHELXTL-Plus*, Release 5.1; Bruker AXS Inc.: Madison, WI, 1997.

(12) Sheldrick, G. M. *SHELX97, Programs for Crystal Structure Analysis*, Release 97-2; University of Göttingen: Göttingen, Germany, 1998.

Table 4. Bond Lengths (Å) and Angles (deg) at Room Temperature[a]

	$RuBr_3$	$MoBr_3$		$RuBr_3$	$MoBr_3$
M−Br(1)	2.518(2)	2.594(2)	M−Br(4)	2.523(4)	2.606(3)
M−Br(2)	2.470(2)	2.561(2)	M−M	2.732(3)	2.874(3)
M−Br(3)	2.471(4)	2.549(3)	M···M	3.127(3)	3.203(3)
Br(1)−M−Br(1′)	85.4(1)	85.94(8)	Br(2)−M−Br(2″)	92.5(1)	91.53(8)
Br(1)−M−Br(2)	90.95(6)	91.20(4)	Br(2)−M−Br(3)	92.31(7)	91.50(6)
Br(1)−M−Br(3)	90.90(9)	91.34(7)	Br(2)−M−Br(4)	90.97(9)	91.02(7)
Br(1)−M−Br(4)	85.62(7)	86.02(6)	Br(3)−M−Br(4)	175.3(1)	176.4(1)
Br(2)−M−Br(1′)	175.20(8)	176.01(7)			

[a] A single prime indicates $x, -y + 1/2, -z - 1/2$; a double prime indicates $x, -y + 1/2, -z + 1/2$.

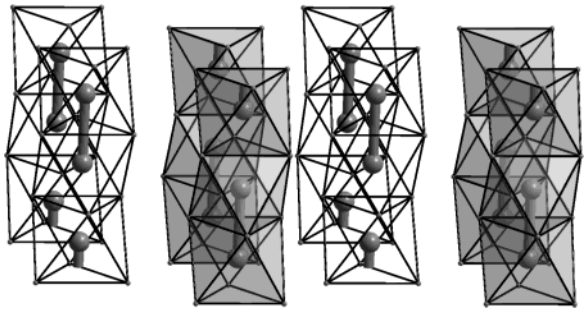

Figure 6. Perspective view of the crystal structure of $RuBr_3$ and $MoBr_3$. The Br atoms are located at the vertexes of the coordination polyhedra. The neighboring rows of chains, presenting the M−M pairs at different heights along **c**, are distinguished by different shadings.

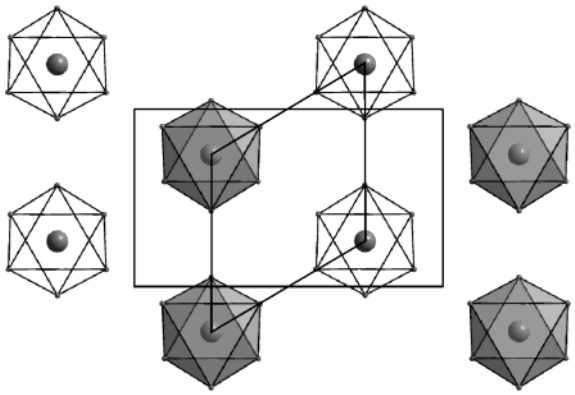

Figure 7. View along **c** of the column layout in the crystal structure of $RuBr_3$ and $MoBr_3$. The columns having the metals at different heights in *c* are distinguished by different shadings. The unit cells for both the disordered (hexagonal) and the ordered (orthorhombic) dispositions of the columns are also shown.

intensities were scaled with respect to the intensities of "reference" structure reflections, 133 and 403, respectively. In the case of the $MoBr_3$ compound the measurements were carried out on the three individuals of the Drilling, for both the superstructure and structure reflections, and their average was used in the subsequent calculations.

At each step, before the intensities of the structure and superstructure reflections were measured (scan width 1°, scan speed 0.5 deg/min), the crystals were kept for 2 h at the selected temperature and afterward recentered (22 structure reflections were used in the recentering process).

The results are given in a deposited table, reporting all the measurements at different temperatures, the average values of the intensities of the superstructure reflections, and the corresponding values rescaled with

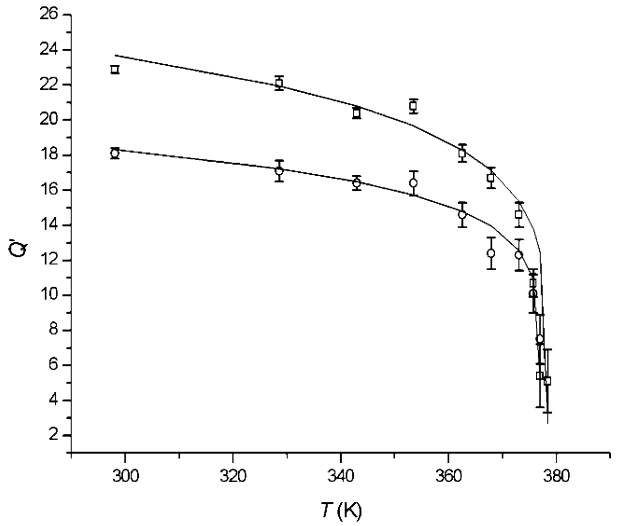

Figure 8. Fitting of Q' experimental values obtained from the intensities of reflections 123, □, and 413, ○, of $RuBr_3$.

Table 5. Thermal Variation of Experimental Order Parameters Q' Calculated from the Intensity of Two Superstructure Reflections

$RuBr_3$			$MoBr_3$	
T (K)	Q'_{123}	Q'_{413}	T (K)	Q'_{123}
298.1	22.9(2)	18.1(3)	298.1	51.1(18)
328.6	22.1(4)	17.1(6)	353.5	51.4(18)
343.0	20.4(3)	16.4(4)	373.1	49.0(19)
353.5	20.8(4)	16.8(7)	392.8	49.3(19)
362.6	18.1(5)	14.6(7)	403.2	49.3(19)
367.9	16.7(6)	12.4(9)	413.7	46.7(20)
373.1	14.6(7)	12.3(9)	416.3	45.9(20)
375.7	10.7(8)	10.1(11)	418.9	49.0(19)
377.0	5.4(18)	7.5(14)	424.2	47.5(20)
378.4	5.1(18)		428.1	47.5(20)
			434.7	44.8(21)
			441.2	45.1(21)
			447.7	43.2(22)
			454.3	40.2(23)
			458.2	36.0(26)
			462.2	27.2(33)
			466.1	17.6(50)

respect to the reference structure reflections. The macroscopic order parameter Q is related to the intensity of a superstructure reflection: $Q \propto Q' = \sqrt{I}$. The Q' values, calculated from the intensities (of the superstructure reflections) I_{123} and I_{413} for $RuBr_3$ and I_{123} for $MoBr_3$ at various temperatures, are presented in Table 5. The variation of Q' with temperature is expressed as

$$Q' = k|T - T_c|^{\beta} \qquad (1)$$

Figure 8 presents the variation of Q' with T for $RuBr_3$, determined from the measurements of the

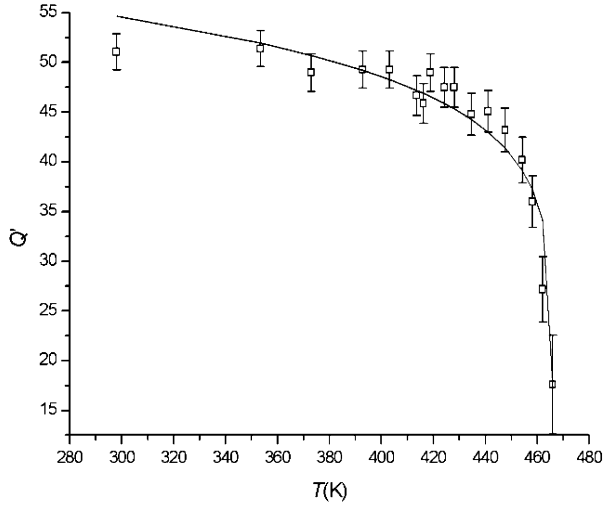

Figure 9. Fitting of Q' experimental values obtained from the intensity of reflection 123 of $MoBr_3$.

Table 6. Best Fitting Parameters of Q' Values vs Temperature

	refln	k	T_c (K)	β
$RuBr_3$	123	12.8(12)	378.4(13)	0.129(25)
	413	10.3(7)	377.1(9)	0.125(15)
$MoBr_3$	123	29.8(19)	466.1(9)	0.115(16)

intensities of the reflections 123 and 413; Figure 9 presents the variation of Q' for $MoBr_3$, determined from the measurements of the intensity of the reflection 123. Table 6 presents the best fitting parameters for expression 1.

The values reported in Table 6 indicate the transition temperatures for $RuBr_3$ (377.5 K, by averaging the values obtained from the two high-temperature studies on 123 and 413 reflections) and $MoBr_3$ (466.1 K), and are used to derive the order parameter $Q = Q'/(kT_c^{\beta})$.

Finally, a full data collection at a temperature of 105 °C, slightly higher than T_c, was carried out with the $RuBr_3$ crystal, and a structure refinement was performed in the space group $P6_3/mcm$, corresponding to the symmetry displayed by the crystal at that temperature.

We thought it would be instructive to carry out a parallel refinement, in the space group $P6_3/mcm$, using only the structure reflections ($h + k = 2n$) selected from the whole set of data collected at room temperature. The crystal data and some details of the two structure refinements are presented in Table 7, whereas the positional and thermal parameters obtained as results of the two refinements are compared in Table 8.

If the high-temperature structure would correspond to a situation in which Ru and Br atoms are in ordered positions, with equidistant metal atoms and equivalent anion triangles in each column, then we should register anisotropic thermal parameters U_{33} for Ru and U_{11} and U_{22} for Br well lower than the corresponding values obtained in the refinement carried out with only structure reflections collected at room temperature. In fact, the structure presents in each column, at room temperature, alternating short and long metal−metal distances, as well as an ordered sequence of "large" and "small" triangles; therefore, the atomic positions presented in Table 8 correspond to the average position of the Ru atoms (which actually lie in two positions ∼0.20 Å apart) and of the Br atoms (actually lying in two positions ∼0.10 Å apart).

Other considerations may be put forward to disprove the assumption that in the orthorhombic form the metal−metal distances are a continuous function of the temperature, with decreasing difference between the lengths of M−M and M···M bonds with rising temperature, finally yielding the hexagonal form, with equally spaced metal atoms in each column. In this approach to the phase transformation, the structural arrangements should be well ordered at all temperatures, whereas the variation of the superstructure reflection intensities with T are consistent with an order−disorder transformation, with the typical character of cooperativity, which increasingly favors the process of transition as the critical temperature is approached.

We may also consider that, at constant total bond order for each metal atom, the equalization of the two bonds with adjacent metal atoms would cause a shorter c parameter, with respect to the "unequal-bond" arrangement. On the other side, if we assume that the total bond order decreases with increasing temperature, we should observe a c parameter sensibly larger in the hexagonal than in the orthorhombic phase. What is highly improbable is that, in both $RuBr_3$ and $MoBr_3$, which present equal c parameters in the two forms, the decrease in the total bond order with rising temperatures is exactly what is needed to compensate for the increasing similarity of the two bonds.

These observations strongly support our model, which assumes that (a) at both high and low temperatures the various columns building up the TiI_3 structure type are internally ordered in the **c** direction, both in the alternating short M−M and long M···M bonds and in the corresponding ordered sequence of large and small triangles of halide anions, (b) two distinct, although geometrically and energetically equivalent, ordering schemes exist, indicated as + and − in the Introduction, with columns + and − disposed in a regular arrangement on a triangular lattice, and (c) at temperatures higher than T_c no correlation exists among the ordering schemes assumed by the various columns and the

Table 7. Comparison of Crystal Data and Structure Refinement of $RuBr_3$ for the Structure Reflections at Room Temperature (RT) and for the Whole Set of Hexagonal Reflections at High Temperature (378 K)

	RT	378 K		RT	378 K
wavelength (Å)	0.71073	0.71073	no. of reflns collected	348	324
space group	$P6_3/mcm$	$P6_3/mcm$	no. of independent reflns	95 (R_{int} = 0.093)	89 (R_{int} = 0.127)
a (Å)	6.488(1)	6.499(1)	no. of independent reflns [$I > 2\sigma(I)$]	80	70
b (Å)	6.488(1)	6.499(1)	no. of refined params	8	8
c (Å)	5.859(1)	5.871(2)	GOF	0.497	1.359
V (Å^3)	427.07(16)	459.25(11)	R1, wR2 [$I > 2\sigma(I)$]	0.035, 0.085	0.116, 0.248
ρ_{calcd} (g·cm^{-3})	5.30	5.27	R1, wR2 (all data)	0.043, 0.101	0.146, 0.274
μ (mm^{-1})	31.51	31.33	max peak and hole in ΔF (e·Å^{-3})	0.94/−1.18	1.91/−2.33

Table 8. Atomic Coordinates, Equivalent Isotropic (Å^3) and Anisotropic (Å^2) Displacement Parameters of $RuBr_3$, Obtained with Structure Reflections at RT and for the Hexagonal Structure at 105 °C (378 K)

		RT	378 K			RT	378 K
Ru	*x*/*a*	0	0	Br	*x*/*a*	0.3107(3)	0.3115(11)
	y/*b*	0	0		*y*/*b*	0.3107(3)	0.3115(11)
	z/*c*	0	0		*z*/*c*	1/4	1/4
	U_{eq}	0.022(1)	0.024(3)		U_{eq}	0.024(1)	0.031(3)
	U_{11}	0.020(1)	0.018(3)		U_{11}	0.025(1)	0.033(3)
	U_{22}	0.020(1)	0.018(3)		U_{22}	0.025(1)	0.033(3)
	U_{33}	0.027(2)	0.035(7)		U_{33}	0.018(2)	0.021(5)
	U_{23}	0	0		U_{23}	0	0
	U_{13}	0	0		U_{13}	0	0
	U_{12}	0.010(1)	0.009(2)		U_{12}	0.008(1)	0.011(3)

crystals present the space group symmetry $P6_3/mcm$, whereas at temperatures lower than T_c that correlation exists and long-range order sets up and increases with decreasing temperature, reaching, in the limit of 0 K, the structural arrangement described by Figures 6 and 7.

In fact, a refinement carried out with the data collected at 378 K for the $RuBr_3$ compound, assuming the model just described (atoms in fixed positions: Ru at 0.0, 0.0, 0.0168; Br(1) at 0.3172, 0.3172, 1/4; Br(2) at 0.3008, 0.3008, 1/4), resulted in better agreement factors (R1[$I > 2\sigma(I)$] = 0.111; R1(all data) = 0.139; wR2 = 0.225) and well lower residual peaks (0.91/−1.37) than those obtained (Table 7) with the model presenting equidistant metal atoms and equivalent anion triangles.

5. Ising Model

Figures 3 and 4 suggest that we may neglect one of the lattice dimensions and describe the TiI_3 structure type as a two-dimensional Ising system. The Ising model, first developed to describe magnetic systems considering only the local interactions between magnetic spins, was later fruitfully applied to order−disorder phenomena in alloys and, more generally, in inorganic compounds. Also in these cases the term "spin" has been retained, but it does not refer to any magnetic properties: it is simply a variable which can assume one of two values (spin-1/2 Ising models) as in the system under discussion, or one of more values (higher-spin Ising models);[13] similarly the terms "ferromagnetic" and "antiferromagnetic" interactions are retained with the meaning that similar or opposite spins, respectively, tend to occur as next neighbors.

In a triangular lattice, such as that corresponding to the two-dimensional distribution of the columns in the TiI_3 structure type, it is not possible for a + spin to have only − spins as nearest neighbors (and vice versa), a peculiar situation known as "frustration". The term has been introduced in the study of antiferromagnetic systems to indicate the impossibility to obtain a minimum-energy configuration with antiparallel orientation of every pair of adjacent magnetic spins. Wannier showed that the ground state in a triangular lattice with only antiferromagnetic interactions between nearest neighbor (*nn*) spins is highly degenerate, so that no long-range ordering occurs.[14] To remove the degeneracy and

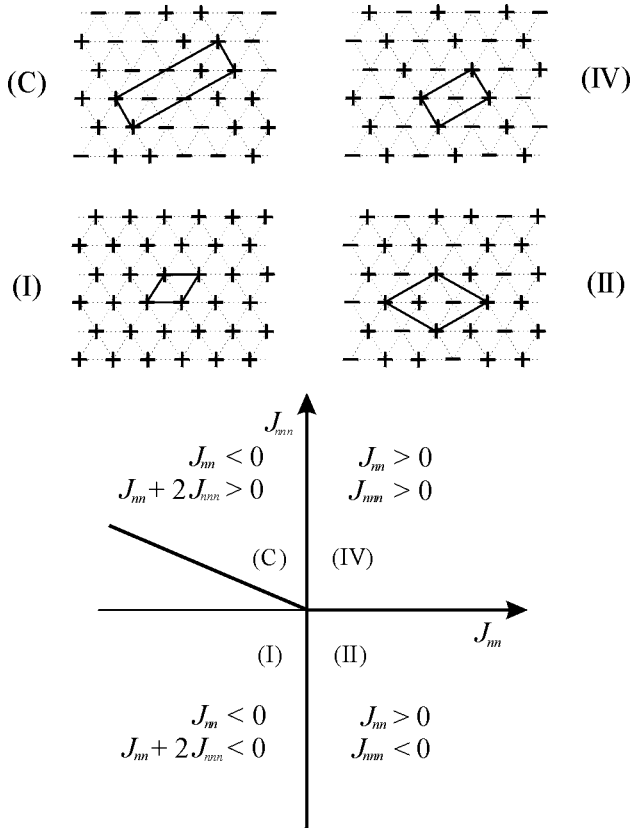

Figure 10. Possible spin orderings in a triangular net, following Tanaka and Uryû.

confer stability to particular structures, weak interactions between next-nearest neighbors (*nnn*) have to be introduced. Metcalf[15] and Tanaka and Uryû[16] discussed the ground-state ordering ($T = 0$ K) in a triangular Ising model with *nn* and *nnn* interactions, assuming various ratios and signs for the *nn* and *nnn* interaction strengths.

The proper Hamiltonian in the case under study can be written as

$$H = J_{nn}\sum_{nn}\sigma_i\sigma_j + J_{nnn}\sum_{nnn}\sigma_i\sigma_k$$

where σ is a two-value variable (+1 or −1, depending on the ordering scheme of the corresponding column), J_{nn} is the difference between the interaction energy for *nn* columns with the same ordering scheme and the interaction energy of *nn* columns with opposite ordering scheme, and J_{nnn} is the same for *nnn* columns.

Tanaka and Uryû[16] found four distinct spin orderings: the structures and their positions within the phase diagram in (J_{nn}, J_{nnn}) space are presented in Figure 10. Structure IV closely corresponds to the TiI_3 structure type. Consequently, we may assume that the same physical situation occurs in our compounds, namely, that both the *nn* and *nnn* interactions are of antiferromagnetic type.

The substantial two-dimensionality of this structural arrangement is dependent on the strong internal correlation of the atomic positions in each column, which may be ordered in one way or in the opposite way. Moreover, the switching from one to the other confor-

(13) Yeomans, J. M. *Statistical mechanics of phase transitions*, Clarendon Press: Oxford, U.K., 1992.

(14) Wannier, G. H. *Phys. Rev.* **1950**, *79*, 357.
(15) Metcalf, B. D. *Phys. Lett.* **1974**, *46A*, 325.
(16) Tanaka, Y.; Uryû, N. *J. Phys. Soc. Jpn.* **1975**, *39*, 825.

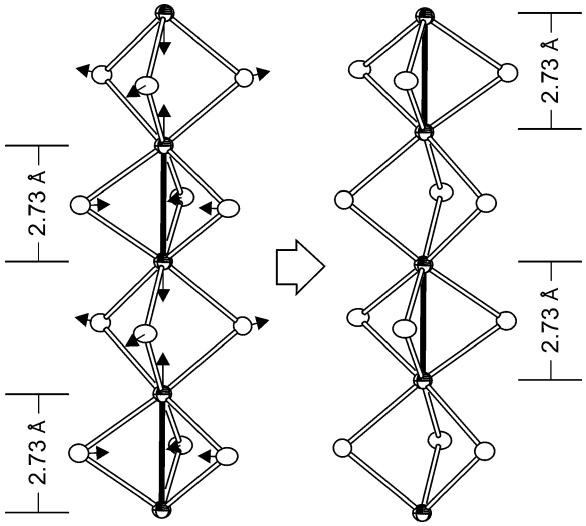

Figure 11. Atomic movements which drive the transformation of a "+"-type column into a "−"-type one.

Table 9. M−M and M···M Distances (Å) in the Structural Columns: (a) Values Obtained by Extrapolating at 0 K the δ_M Values at 298 K; (b) Values Obtained from Refinements Carried out with the Data Collected at Room Temperature, Using Only the Reflections with $h + k = 2n + 1$

	$RuBr_3$		$MoBr_3$	
	a	b	a	b
M−M	2.69	2.68	2.84	2.85
M···M	3.17	3.18	3.23	3.22

mation is easy and does not require any appreciable activation energy. The movements of atoms which start the inversion of conformation are schematically presented in Figure 11, which clearly shows the concerted movements and explains how the changes in one pair of metal atoms propagates through the whole column. Understandably, the order−disorder process is reversible: we have checked this point by fully disordering the crystals of $RuBr_3$ and $MoBr_3$ and afterward lowering the temperature at various values below T_c; we obtained, by measuring the intensities of the 123 reflections, the same Q values obtained, at those temperatures, in the step-by-step heating experiments.

As the equalization of the bond distances in the metal chains of each column is an artifact depending on the random distribution of the two kinds of chain conformations, the various degrees of disorder affect the values of bond distances obtained at low temperatures, and the measured "apparent" differences (δ_M) in the M−M and M···M distances vary as the order parameter. The actual difference, corrected for the random distribution of part of the columns, is that calculated for $Q = 1$ ($T = 0$ K).

At room temperature the $Q = Q'/(kT_c^{\beta})$ values were 0.835 for $RuBr_3$ and 0.845 for $MoBr_3$, which means that nearly 8% of the vertexes of the triangular net in Figure 4 are randomly occupied by + and − columns. δ_{Ru} and δ_{Mo} are 0.394 and 0.328 Å at 298 K. The corresponding values at 0 K may be easily obtained as $\delta_{Ru}(0\text{ K}) = 0.472$ Å and $\delta_{Mo}(0\text{ K}) = 0.388$ Å. From these values we obtain the actual distances M−M and M···M in the columns, valid at all temperatures and reported in Table 9.

It is interesting to observe that from the refinements carried out with the data collected at room temperature, using only the superstructure reflections, namely after elimination of the reflections with $h + k = 2n$, the only ones which convey the contribution of the disordered part of the structure, we obtained, for both $RuBr_3$ and $MoBr_3$, M−M and M···M distances similar to those obtained by extrapolating at 0 K the δ_M values at 298 K, as shown in Table 9.

6. Conclusions

The results of the structural investigations carried out on crystals of $RuBr_3$ and $MoBr_3$ at room and high temperatures indicate that these two compounds with the TiI_3 structure type present two different forms, a hexagonal form with space group $P6_3/mcm$ and an orthorhombic one, with space group $Pnmm$. In both forms columns of $[MX_6]$ octahedra run along **c**, displaying regular alternation of M−M and M···M pairs, with short and long distances, respectively. The columns may have two distinct conformations, namely conformation +, in which M−M pairs are centered at $z = 1/4$, and conformation −, in which M−M pairs are centered at $z = 3/4$. In the orthorhombic form the distribution of the two types of columns in the **a**,**b** plane is largely ordered, perfectly ordered at $T = 0$ K. The disorder in the distribution of the types of columns increases with increasing temperature, and the degree of order is given by $Q = |(T - T_c)/T_c|^{\beta}$, with $Q = 0$ at the critical temperature T_c (T_c is 377.5 and 466 K for $RuBr_3$ and $MoBr_3$, respectively) and $Q = 1$ at $T = 0$ K.

The order−disorder character of the process is in agreement with the kind of variation of Q as a function of temperature. On the other side the substantial two-dimensionality of the system is in keeping with the relatively low values of the critical exponent β obtained in the heating studies carried out on $RuBr_3$ and $MoBr_3$ crystals. The system seemingly conforms to a two-dimensional "triangular-net" Ising model, with frustration removed by the introduction of *nnn* interactions between columns.

Presumably, not only $RuBr_3$ and $MoBr_3$ but all the trihalides of the III−V transition metals crystallizing in the structure type of TiI_3 and characterized by infinite columns of confacial $[MX_6]$ octahedra running along **c** display the same features we have presented and discussed for $RuBr_3$ and $MoBr_3$. However, at room temperature the different compounds present different extents of ordering in the distribution of the two types of column conformations in the **a**,**b** plane. When the distribution is fully disordered (or, at least, highly disordered) the structure will appear hexagonal with $P6_3/mcm$ symmetry and apparent equalization of the distances between the M atoms along the columns; an ordered arrangement of the columns may be recovered by properly lowering the temperature. On the other side, when the distribution of the column types is largely ordered, the structure will appear orthorhombic with $Pnmm$ symmetry. Also in this case, partial disorder persists and $\delta_M = d_{M\cdots M} - d_{M-M}$ is partially affected by disorder; the actual degree of order Q may be evaluated by measuring the intensities of the superstructure reflections at various T values and determining the critical temperature T_c and the critical exponent β. Once these values are known, the actual values of the alternating short and long intermetal distances in the columns may be derived.

We plan to extend our investigations to other compounds in this family and to carry out the study of their thermal behavior not only at high but also at low temperatures; in this way a reliable pattern of correlations between chemical compositions and critical temperatures could be established and the driving forces of this kind of order−disorder transformation properly understood.

Acknowledgment. We thank Prof. G. Fachinetti for the gift of an amount of $Ru_3(CO)_{12}$, Prof. F. Calderazzo and D. Belli Dell'Amico for helpful discussions, and the following institutions for financial support: University of Pisa, Ministero dell' Istruzione, dell' Università e della Ricerca (MIUR), Programmi di Ricerca Scientifica di Rilevante Interesse Nazionale, 2001 and 2002, and Consiglio Nazionale delle Ricerche, Progetto CNR/MIUR "Sviluppo di Microcelle a Combustibile".

Supporting Information Available: Crystallographic data for the RT refinements of $RuBr_3$ and $MoBr_3$ in the orthorhombic setting, for the RT refinement of $RuBr_3$ in the hexagonal setting, and for the HT refinement of $RuBr_3$ (CIF). This material is available free of charge via the Internet at http://pubs.acs.org. Additionally, the same data have been deposited with the Fachinformationszentrum (FIZ) Karlsruhe, Germany (CSD Nos. 413689, 413690, 413691, and 413692).

CM049235Q